PCCP

PAPER

Body-centered tetragonal B_2N_2: a novel sp^3 bonding boron nitride polymorph

Bin Wen,*[a] Jijun Zhao,[b] Roderick Melnik[c] and Yongjun Tian[a]

A novel polymorph of boron nitride (BN) with a body-centered tetragonal structure (bct-BN) has been predicted using first-principles calculations. The structural, vibrational, and mechanical calculations indicated that bct-BN is mechanically stable at zero pressure. When pressure is above 6 GPa, bct-BN becomes energetically more stable than h-BN. The bct-BN appears to be an intermediate phase between h-BN and w-BN due to a low energy barrier from h-BN to w-BN via bct-BN. Our results also indicated that the structure of unknown E-BN phase might be bct-BN.

I. Introduction

Attributed to their specific atomic bonding, boron nitride (BN) can form many polymorphs,[1] such as hexagonal BN (h-BN),[2] zinc blende BN (c-BN),[3] wurtzite BN (w-BN),[4] 5H-BN,[5] amorphous BN,[6] BN nanotubes,[7] and BN nanomesh.[8] Structurally and characteristically similar to graphite and diamond respectively,[5] h-BN and c-BN have been receiving considerable attention due to their excellent optical, electrical, and mechanical properties.[1] Because these polymorphs differ significantly in both electronic and mechanical properties, phase transformations between various forms of BN have long been a topic of interest, and numerous theoretical[9–14] and experimental[4,15–20] efforts have been devoted to elucidate the transformation mechanisms between various forms of BN.

Despite these efforts, the transformation mechanism between the h-BN and w-BN phases is still a puzzling question. Although c-BN is the energetically stable phase at pressure beyond 6 GPa[10] at room temperature with respect to w-BN and h-BN, only w-BN has been synthesized to date by cold compressing h-BN.[17] However, the experimental phase transformation pressure (about 15 GPa)[17] is substantially higher than the theoretically predicted value of 6.5 GPa.[10] To understand the transition from h-BN to w-BN, a new transformation mechanism has been suggested recently based on accurate inelastic X-ray scattering experiments and recent first-principles calculations by Meng et al.[17] and Wang et al.[14] They argued that h-BN layers get close together; each N atom

[a] State Key Laboratory of Metastable Materials, Science and Technology, Yanshan University, Qinhuangdao 066004, China. E-mail: wenbin@ysu.edu.cn
[b] Key Laboratory of Materials Modification by Laser, Ion and Electron Beams, Dalian University of Technology, Ministry of Education, Dalian 116024, P. R. China
[c] M²NeT Lab, Wilfrid Laurier University, Waterloo, 75 University Ave. West, Ontario, Canada N2L 3C5

in a hexagonal layer buckles down in the c-axis direction and forms bonds with a B atom directly below it in an adjacent layer.[14] However, considering a B atom and an adjacent N atom as a B–N pair, and a half of these B–N pairs buckle down in the c-axis to form two bonds with the adjacent layer's pair, the energy barrier will be roughly similar due to the same number of broken bonds for these two transformation mechanisms. This implies coexistence of another new phase with w-BN during the experimental procedures to synthesize w-BN from h-BN.

To further understand the transformation mechanism from h-BN to w-BN and verify our hypothesis, a novel polymorph of BN with a body-centered tetragonal (space group: $P42/mnm$) structure (bct-BN)[21–24] has been built in this work. A low energy barrier path from h-BN to w-BN via bct-BN was found, indicating that bct-BN may be an intermediate phase from h-BN to w-BN. Our results also imply that the structure of an unknown E-BN phase might be bct-BN.

II. Computational method

The crystal cell parameters and atomic positions of different BN polymorphs under high pressures have been optimized by using density functional theory (DFT) based on the planewave pseudopotential technique implemented in the CASTEP package,[25] and the corresponding enthalpies have been computed. The ion–electron interaction is modeled by norm-conserving pseudopotentials.[26] The electron exchange correlation energy is described in the local density approximation (LDA).[27,28] The kinetic cutoff energy for plane waves is set as 770 eV. The **k** point separation in the Brillouin zone of the reciprocal space is 0.04 nm^{-1}, resulting in different **k** point meshes, i.e., $6 \times 6 \times 10$ for bct-BN, $12 \times 12 \times 4$ for h-BN, $8 \times 8 \times 8$ for c-BN, $11 \times 11 \times 6$ for w-BN, and $3 \times 10 \times 6$ for M-BN, respectively.

Benchmark calculations were conducted for c-BN phase to validate our computational scheme. The calculated lattice parameter of 0.3589 nm compares well with the experimental value of 0.3620 nm.[4] The computed elastic constants for the c-BN phase are $C_{11} = 799$ GPa, $C_{44} = 467$ GPa, and $C_{12} = 170$ GPa. They are also in reasonable agreement with the experimental values of $C_{11} = 820$ GPa, $C_{44} = 480$ GPa, and $C_{12} = 190$ GPa.[29]

III. Results and discussion

In this work, bct-BN has been constructed by compressing h-BN along the c-axis and then moving half of the B–N pair toward the adjacent layer's pairs. Views along the [100]/[001] direction and [010] direction of the $2 \times 2 \times 2$ supercell of bct-BN are shown in Fig. 1a and b, respectively. The initial crystal structures of h-BN, c-BN, and w-BN were taken from the experimental crystallographic data in ref. 1–4. The initial crystal structure M-BN was built by imitating M-carbon.[22–24] The lattice parameters and internal coordinates of the five polymorphs were optimized by using first-principles with symmetry constraint. The calculated values of lattice parameters, and the corresponding relative total energy at 0 GPa,
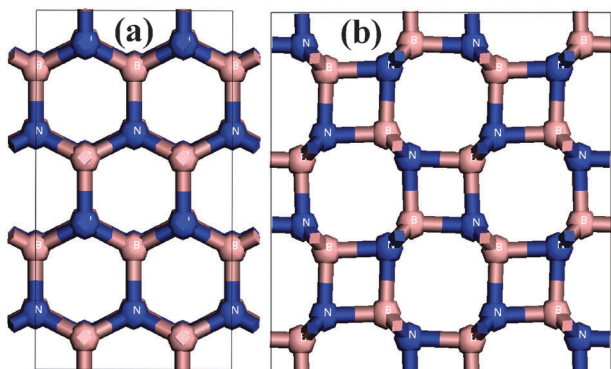
together with the available experimental and calculated data are shown in Table 1. As can been seen from Table 1, at ambient conditions, c-BN is the most stable phase, and h-BN is a metastable phase. This result agrees well with Kern's computational[12] and Sachdev's experimental results.[30] Although
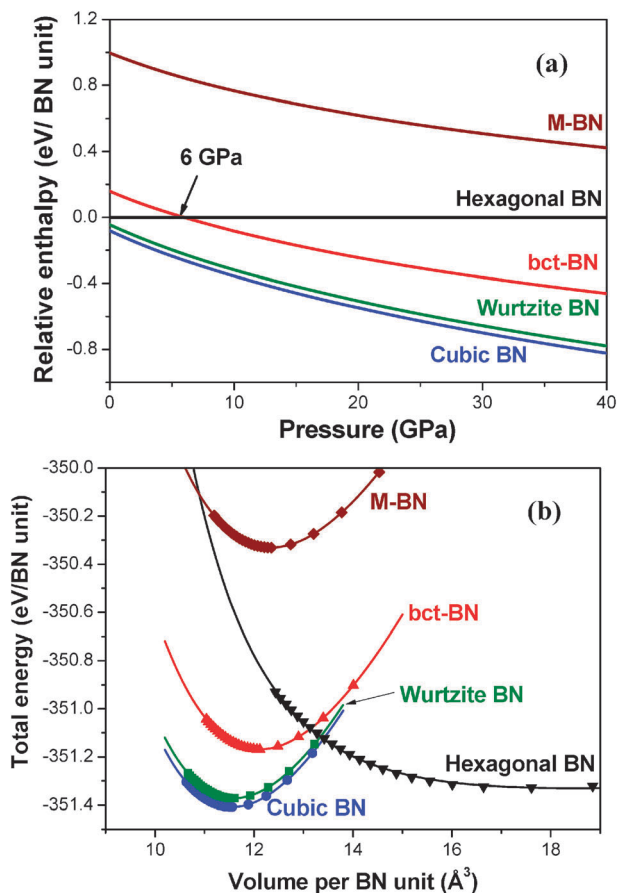

Fig. 2 (a) Relative enthalpies of bct-BN, M-BN, wurtzite BN, and cubic BN with respect to hexagonal BN. (b) Total energy *versus* volume for bct-BN, M-BN, wurtzite BN, cubic BN and hexagonal BN, the curves are fitted using Murnaghan's equation of state.[32]

Fig. 1 Views along [100]/[001] direction (a) and along [010] direction (b) of $2 \times 2 \times 2$ supercell of bct-BN.

Table 1 Optimized crystallographic data and relative total energy of boron nitride polytypes at a pressure of 0 GPa

Phases	Space group	Lattice parameters (Å)	Bond length (Å)	Volume (Å³/BN)	Coordination	Total energy (eV/BN)	Bulk modulus (GPa)	Reference
bct-BN	*P*42/*mnm*	$a = c = 4.380, b = 2.526$	1.587	12.117	4	0.159	360.46	This work
M-BN	*Cm*	$a = 9.378, b = 2.542, c = 4.168$	1.525 1.533 1.662	12.348	4	0.996	337.11	This work
h-BN	*P*63/*mmc*	$a = b = 2.489, c = 6.561$ $a = b = 2.494, c = 6.66$	1.437	17.607	3	0	14.09	This work Experimental[a]
w- BN	*P*63*mc*	$a = b = 2.538, c = 4.197$ $a = b = 2.55, c = 4.20$ $a = b = 2.553, c = 4.228$	1.568	11.600	4	−0.044	387.20	This work Experimental[b] Calculated[c]
c-BN	$F\bar{4}3m$	$a = 3.589$ $a = 3.62$ $a = 3.616$	1.554	11.564	4	−0.080	387.28	This work Experimental[b] Calculated[c]

[a] Ref. 10. [b] Ref. 4. [c] Ref. 18.

the LDA functional does not include Van der Waals dispersion energy, the stacking of BN hexagonal layers can be stable at ambient pressure by using present LDA calculations. The optimized lattice parameter c = 6.561 Å at 0 GPa agrees well with the experimental value of 6.66 Å,[4] this confirmed that Van der Waals dispersion energy can be ignored in present calculations. Two different kinds of B–N bonds exist in bct-BN, and there are half with a bond length of 1.587 Å, and half with a bond length of 1.525 Å at ambient pressure. The average bond length is 1.556 Å, which is comparable with c-BN of 1.554 Å. The overlap populations are 0.77 and 0.61 for the two different bonds of bct-BN. The average overlap population of two B–N bonds is 0.64, which is comparable with c-BN of 0.643. The calculated Phillips ionicities are 0.227 and 0.266 for the two different bonds of bct-BN. The Phillips ionicity of two B–N bonds is 0.247, which is comparable with c-BN of 0.256. The results imply that bct-BN should have bond strengths similar to that of c-BN.

Thermodynamical relative stability of BN polymorphs can be studied by comparing the corresponding Gibbs free energy $G = E + PV - TS$, where E is total energy, P is pressure, V is volume, T is temperature and S is entropy. Since no temperature effects are considered in this work, the pressure dependent phase stability of BN polymorphs can be determined by comparing the relative enthalpies $H = E + PV$.[31] In particular, the geometries of these BN polymorphs under pressure have been optimized here by using the DFT calculations, and the enthalpies for these optimized BN polytypes under pressure up to 40 GPa have been obtained. The relationships between the enthalpies and pressure for various BN polymorphs are plotted in Fig. 2a. The cubic c-BN is the most energetically favorable phase, w-BN is energetically less favorable with respect to c-BN, but it is more stable than layered h-BN at all pressures considered here. Our results are in excellent agreement with Kern's computational[12] and Sachdev's experimental results.[30] When the pressure is above 6 GPa, bct-BN becomes more stable than h-BN, but less stable with regard to w-BN. In Fig. 2b, the total energy *versus* volume data for bct-BN, M-BN, wurtzite BN, cubic BN and hexagonal BN have also been plotted, and the corresponding bulk moduli
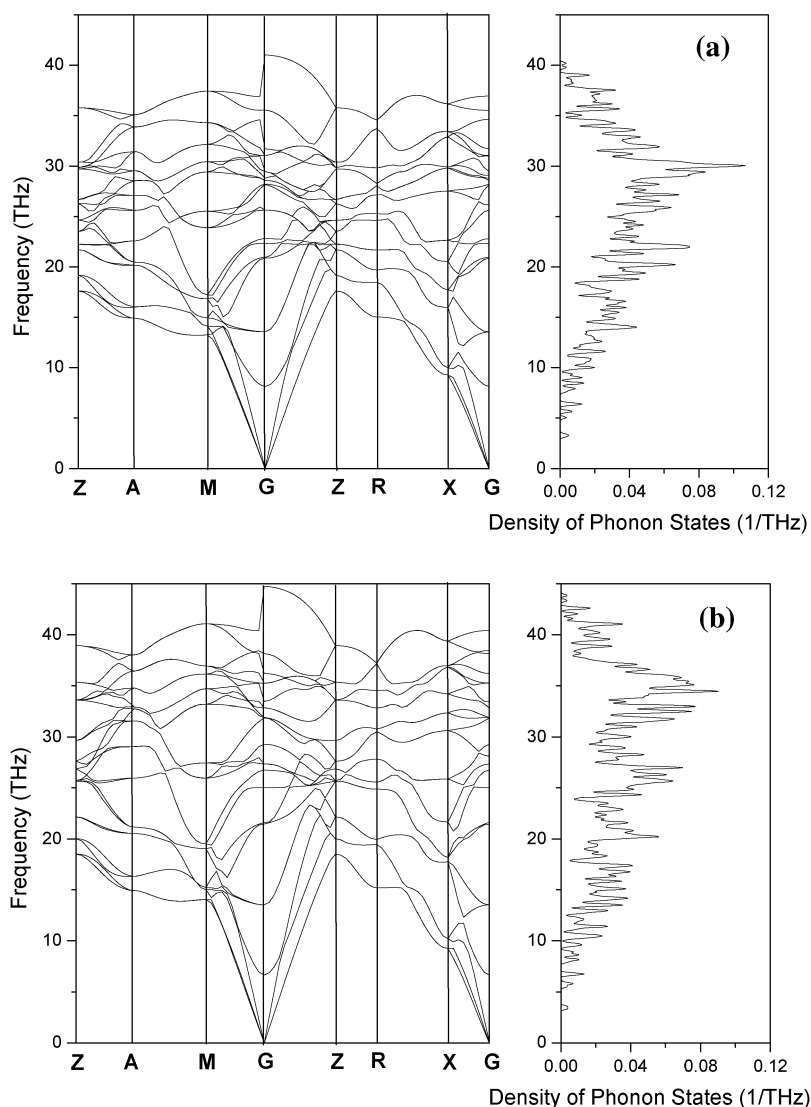

Fig. 3 Calculated phonon band structure (left panel) and density of states (right panel) of bct-BN under pressures of 0 (a) and 40 GPa (b).

have been obtained by fitting with the Murnaghan equation of state,[32] and are listed in Table 1. The bulk modulus of bct-BN is 360.46 GPa, which is comparable with c-BN and w-BN of 387.28 and 387.20 GPa, respectively. The computed phonon dispersions of bct-BN at 0 and 40 GPa indicated that bct-BN is mechanically stable (as shown in Fig. 3). These results suggest that bct-BN is a new metastable phase of BN, and it may be synthesized by compressing the h-BN precursor appropriately.

As we suggested above, bct-BN can be viewed as a metastable intermediate phase between h-BN and w-BN. To confirm this viewpoint, transformation paths from h-BN to w-BN via bct-BN at pressure values of 0, 5, 10 and 15 GPa have been constructed, and the corresponding enthalpy curves along these transformation paths have been calculated and they are presented in Fig. 3. To build the transformation path from h-BN to w-BN via bct-BN, the lattice vectors are redefined as those of a tetragonal lattice based on the original hexagonal lattice of h-BN and w-BN. In other words, the [1$\bar{1}$0] and [110] directions in the hexagonal lattice are redefined as the *a* and *b* directions in the tetragonal lattice, respectively. Thus, the transformation paths can be characterized by an internal parameter ξ. For the transformation path from h-BN to bct-BN, we vary the lattice parameters of h-BN linearly to that of bct-BN. For example, at 15 GPa, the lattice parameters *a*, *b* and *c* can be expressed as a function of the parameter ξ: $a = 4.28 + 0.92\,(\xi - 0.25)$ (in units of Å), $b = 2.47 + 0.54\,(\xi - 0.25)$ (in units of Å) and $c = 5.62 - 19.54\,(\xi - 0.25)$ (in units of Å). When $\xi = 0.25$, the structure is h-BN; for $\xi = 0.31548$, the structure is bct-BN. At each step, we fix the lattice parameters, fully optimize the atomic position at given pressure; then we can obtain the corresponding enthalpy value. Along the transformation path from bct-BN to w-BN, we vary the fractional coordinates of bct-BN linearly to that of w-BN. At each step, we fix the fractional coordinates, and fully optimize the lattice parameter at a given pressure. Then we can obtain the value of enthalpy at this step. For comparison, direct transformation paths from h-BN to w-BN suggested by Wang et al.[14] have also been constructed. As can be seen from Fig. 4, at pressures of 0 and 5 GPa, h-BN is energetically more stable than bct-BN, the transformation from h-BN to bct-BN cannot occur. Although w-BN is energetically more stable than h-BN, the energy barrier from h-BN to w-BN is so high that the phase transformation cannot happen at room temperature, and high energy processing is needed. At pressures of 10 and 15 GPa, bct-BN and w-BN are all energetically more stable than h-BN, and the energy barriers from h-BN to bct-BN and w-BN are nearly similar (about 0.18 eV/BN unit for 10 GPa and 0.13 eV/BN unit for 15 GPa). This implies that the transformation from h-BN to w-BN and bct-BN can happen at room temperature, and w-BN and bct-BN can coexist as final transformation products from h-BN. We also note that the energy barriers from bct-BN to w-BN are in the range of 0.25 to 0.29 eV/BN unit at a pressure range from 0 to 15 GPa. This means that bct-BN may transform into w-BN under a relatively high temperature condition.

Under hydrostatic pressure, it is not easy to maintain bct-BN due to the low energy barrier for transforming into w-BN. However, if the action time of compression is very
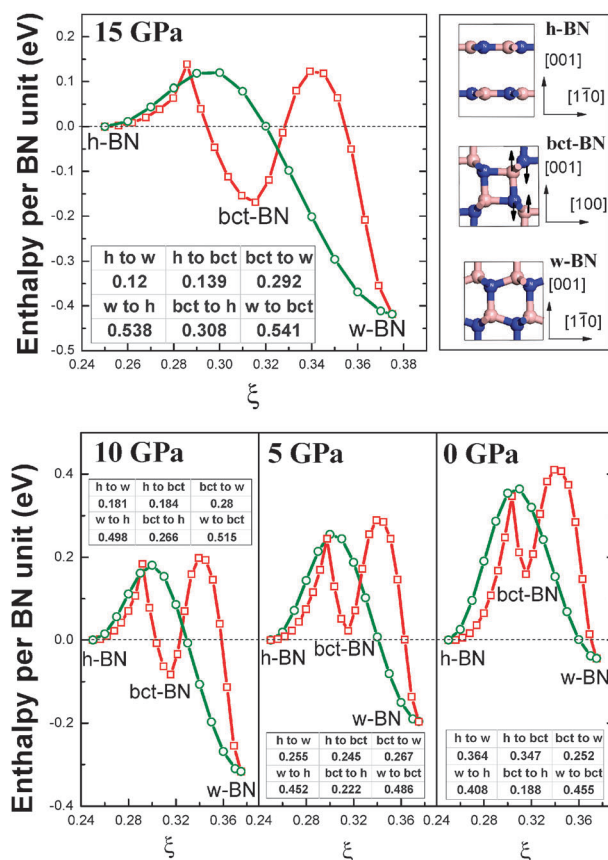

Fig. 4 Energy path from h-BN to w-BN via bct-BN as an intermediate state (squares), and a direct energy path from h-BN to w-BN (circles) under various pressures. Energy barriers (in eV/BN unit) have been listed in the inset tables.

short, like in the case of shock compression, the bct-BN phase may be maintained as a metastable phase at ambient conditions. In an early experiment,[33,34] an unknown BN phase, namely E-BN, has been found as a by-product of w-BN during the pulse plasma[33] and shock compression in the pressure of 60 GPa and a temperature range of 800–2200 K[34,35] procedures. Interestingly, the *d* spacing of bct-BN (3.11, 2.20, 1.96, 1.55, and 1.39 Å) is in excellent agreement with the experimental values (3.22, 2.20, 1.95, 1.54 and 1.35 Å) of E-BN. Therefore, we argue that the experimentally observed E-BN might be the bct-BN phase from our first-principles prediction.

Since bct-BN is built by sp[3] bonds, one may expect that its mechanical properties may be comparable to c-BN. To further study the mechanical properties of bct-BN, the ideal strength has been investigated, and the corresponding stress–strain relationships have been plotted in Fig. 5 together with that of c-BN. As shown in Fig. 5, the calculated tensile and shear strength along the weakest direction [100] and (010)[001] are 47.8 and 68.6 GPa, respectively. The ideal strength of bct-BN along [100] is less than that of c-BN along [111] (62.0 GPa). But the shear strength of bct-BN in the (001)[001] is stronger than that of c-BN in (111)[11$\bar{2}$], and the shear modulus is about 390.21 GPa by fitting this shear strain–stress curve. The inset of Fig. 5 shows a snapshot of bct-BN at the largest shear stress of 68.6 GPa; as can been see from this figure, the broken
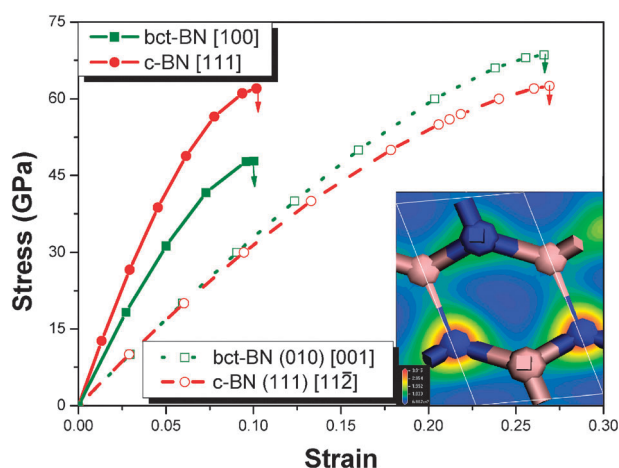
Fig. 5 Calculated stress–strain relationships of bct-BN compared with that of c-BN. The inset shows the electron density of bct-BN in (001) plane at largest shear strain.
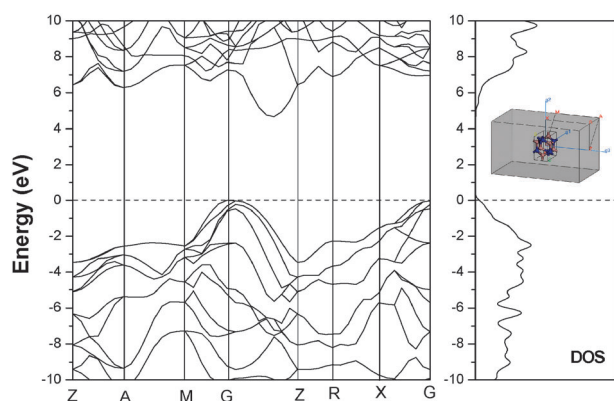

Fig. 6 Calculated electronic band structures of bct-BN at 0 GPa, and the figure on the right shows the first Brillouin zone of the bct-BN.

bond under shear stress is the stronger bond (1.525 Å). This bond is stronger than that of the c-BN B–N bond (1.554 Å); this is the reason that shear strength of bct-BN is stronger than that of c-BN. To further understand the mechanical properties of bct-BN, the Vickers hardness of bct-BN has been calculated by using Tian's method,[36,37] and the calculated Vickers hardness of bct-BN is 65.2 GPa, which is comparable to c-BN (66 GPa).[36–38] The electronic energy band structures of the bct-BN studied here with the corresponding optimized crystal lattices have also been calculated. The results are shown in Fig. 6. According to Fig. 6, bct-BN is an indirect semiconductor with bandgap of 4.676 eV.

IV. Conclusions

In conclusion, a novel polymorph, bct-BN has been proposed, and a lower energy barrier path from h-BN to w-BN through bct-BN has been built, indicating that bct-BN is an intermediate phase from h-BN to w-BN. Calculations of structural, vibrational, and mechanical properties indicated that bct-BN is mechanically stable at 0 and 40 GPa, and more energetically stable than h-BN beyond 6 GPa. Our first-principles calculations

also imply that the experimentally observed E-BN might be the bct-BN phase. These results suggest that the structure of bct-BN is another likely form of a metastable and accessible fourfold-coordinated sp^3 system with appreciable hardness.

References

1 J. J. Pouch and S. A. Alterovitz, Synthesis and Properties of Boron Nitride (Materials Science Forum, Volumes 54–55, 1991).
2 R. T. Paine and C. K. Narula, *Chem. Rev.*, 1990, **90**, 73.
3 P. B. Mirkarimi, K. F. McCarty and D. L. Medlin, *Mater. Sci. Eng., R*, 1997, **21**, 47.
4 F. P. Bundy and R. H. Wentorf, *J. Chem. Phys.*, 1963, **38**, 1144.
5 S. Komatsu, *J. Phys. D: Appl. Phys.*, 2007, **40**, 2320.
6 E. J. M. Hamilton, S. E. Dolan, C. M. Mann, H. O. Colijn, C. A. McDonald and S. G. Shore, *Science*, 1993, **260**, 659.
7 C. Zhi, Y. Bando, C. Tang and D. Golberg, *Materials Science and Engineering*, 2010, **R 70**, 92.
8 M. Corso, W. Auwärter, M. Muntwiler, A. Tamai, T. Greber and J. Osterwalder, *Science*, 2004, **303**, 217.
9 R. M. Wentzcovitch, S. Fahy, M. L. Cohen and S. G. Louie, *Phys. Rev. B*, 1988, **38**, 6191.
10 Y. N. Xu and W. Y. Ching, *Phys. Rev. B: Condens. Matter*, 1991, **44**, 7787.
11 J. Furthmuller, J. Hafner and G. Kresse, *Phys. Rev. B: Condens. Matter*, 1994, **50**, 15606.
12 G. Kern, G. Kresse and J. Hafner, *Phys. Rev. B: Condens. Matter*, 1999, **59**, 8551.
13 Z. Pan, H. Sun, Y. Zhang and C. Chen, *Phys. Rev. Lett.*, 2009, **102**, 055503.
14 H. Wang, Q. Li, T. Cui, Y. Ma and G. Zou, *Solid State Commun.*, 2009, **149**, 843.
15 Q. Johnson and A. C. Mitchell, *Phys. Rev. Lett.*, 1972, **29**, 1369.
16 J. R. Riter, *J. Chem. Phys.*, 1973, **59**, 1538.
17 Y. Meng, H. K. Mao, P. J. Eng, T. P. Trainor, M. Newville, M. Y. Hu, C. Kao, J. Shu, D. Hausermann and R. J. Hemley, *Nat. Mater.*, 2004, **3**, 111.
18 S. P. Gao, J. Zhu and J. Yuan, *Chem. Phys. Lett.*, 2004, **400**, 413.
19 V. I. Levitas, Y. Ma and J. Hashemi, *Appl. Phys. Lett.*, 2005, **86**, 071912.
20 Z. Dong and Y. Song, *J. Phys. Chem. C*, 2010, **114**, 1782.
21 W. L. Mao, H. K. Mao, P. J. Eng, T. P. Trainor, M. Newville, C. C. Kao, D. L. Heinz, J. Shu, Y. Meng and R. J. Hemley, *Science*, 2003, **302**, 425.
22 K. Umemoto, R. M. Wentzcovitch, S. Saito and T. Miyake, *Phys. Rev. Lett.*, 2010, **104**, 125504.
23 X. F. Zhou, G. R. Qian, X. Dong, L. Zhang, Y. Tian and H. T. Wang, *Phys. Rev. B: Condens. Matter Mater. Phys.*, 2010, **82**, 134126.
24 Q. Li, Y. Ma, A. R. Oganov, Hongbo Wang, Hui Wang, Y. Xu, T. Cui, H. K. Mao and G. Zou, *Phys. Rev. Lett.*, 2009, **102**, 175506.
25 S. J. Clark, M. D. Segall, C. J. Pickard, P. J. Hasnip, M. J. Probert, K. Refson and M. C. Payne, *Z. Kristallogr.*, 2005, **220**, 567.
26 D. R. Hamann, M. Schluter and C. Chiang, *Phys. Rev. Lett.*, 1979, **43**, 1494.
27 D. M. Ceperley and B. J. Alder, *Phys. Rev. Lett.*, 1980, **45**, 566.
28 J. P. Perdew and A. Zunger, *Phys. Rev. B*, 1981, **23**, 5048.
29 M. Grimsditch, E. S. Zouboulis and A. Polian, *J. Appl. Phys.*, 1994, **76**, 832.

30 H. Sachdev, R. Haubner, H. Nöth and B. Lux, *Diamond Relat. Mater.*, 1997, **6**, 286.
31 B. Wen and R. V. N. Melnik, *Appl. Phys. Lett.*, 2008, **92**, 261911.
32 F. D. Murnaghan, *Am. J. Math.*, 1937, **49**, 235.
33 A. Rusek, M. Sokolowski and A. Sokolowka, *Journal of Materials Science Letters*, 1981, **16**, 2021.
34 A. Olszyna and I. Zacharenko, *Surf. Coat. Technol.*, 1996, **78**, 227.
35 T. Akashi, A. Sawaoka, S. Saito and M. Araki, *Jpn. J. Appl. Phys.*, 1976, **14**, 891.
36 F. Gao, J. He, E. Wu, S. Liu, D. Yu, D. Li, S. Zhang and Y. Tian, *Phys. Rev. Lett.*, 2003, **91**, 015502.
37 J. He, E. Wu, H. Wang, R. Liu and Y. Tian, *Phys. Rev. Lett.*, 2005, **94**, 015504.
38 Z. Pan, H. Sun, Y. Zhang and C. Chen, *Phys. Rev. Lett.*, 2009, **102**, 055503.